



# Controls of Wind-Driven Jet on the Distribution of Pelagic Cnidarians in the Midwestern South China Sea

Ruping Ge<sup>1</sup>, Hongju Chen<sup>1,2\*</sup>, Ling Li<sup>1,3</sup>, Guangxing Liu<sup>1,2</sup>, Bangqin Huang<sup>4</sup>, Lisha Wang<sup>5</sup>, Yunyun Zhuang<sup>1,2</sup> and Xin Liu<sup>4</sup>

<sup>1</sup> Key Laboratory of Marine Environment and Ecology, Ministry of Education, Ocean University of China, Qingdao, China, <sup>2</sup> Marine Ecology and Environmental Science Laboratory, Pilot National Laboratory for Marine Science and Technology, Qingdao, China, <sup>3</sup> College of the Environment and Ecology, Xiamen University, Xiamen, China, <sup>4</sup> State Key Laboratory of Marine Environmental Science, Xiamen University, Xiamen, China, <sup>5</sup> College of Chemistry and Chemical Engineering, Ocean University of China, Qingdao, China

## OPEN ACCESS

### Edited by:

Dongyan Liu,  
East China Normal University, China

### Reviewed by:

Yuntao Wang,  
Second Institute of Oceanography,  
Ministry of Natural Resources, China  
Tzong-Yueh Chen,  
National Taiwan Ocean University,  
Taiwan

### \*Correspondence:

Hongju Chen  
hongju@ouc.edu.cn

### Specialty section:

This article was submitted to  
Marine Ecosystem Ecology,  
a section of the journal  
Frontiers in Marine Science

**Received:** 18 August 2021

**Accepted:** 29 October 2021

**Published:** 26 November 2021

### Citation:

Ge R, Chen H, Li L, Liu G,  
Huang B, Wang L, Zhuang Y and  
Liu X (2021) Controls of Wind-Driven  
Jet on the Distribution of Pelagic  
Cnidarians in the Midwestern South  
China Sea. *Front. Mar. Sci.* 8:760371.  
doi: 10.3389/fmars.2021.760371

The coastal water transported by the combined action of southwest wind jet and anticyclonic eddy substantially influences the biological processes in the midwestern South China Sea. However, how the wind-driven jet affects the zooplankton community remains unclear. In this study, the species number, abundance, and vertical distribution of medusae were investigated in the wind-driven jet (WJR) and non-wind-driven jet regions (NWJR). The low-salinity and nutrient-rich coastal water substantially influenced species composition, abundance, and vertical distribution of medusae in the WJR. The species number of the meroplanktonic hydromedusae in the WJR was approximately twice that in the NWJR due to the horizontal transport of wind-driven jets. The abundances of holoplanktonic hydromedusae in WJR were  $38.2 \pm 9.3 \text{ ind}\cdot\text{m}^{-3}$ , which were thrice of that in the NWJR regions, caused by the abundant diet in the WJR. Additionally, only the abundance of medusae above the thermocline was affected by the coastal water in WJR, while these showed no significant difference below the thermocline between the WJR and the NWJR. Generalized additive model analyses suggested that the diet was the most important factor affecting the abundance of the holoplanktonic hydromedusae and siphonophore, whereas meroplanktonic hydromedusae were influenced by the combination of temperature, salinity, and diet.

**Keywords:** medusae, vertical distribution, environmental factors, wind-driven jet, community structure

## INTRODUCTION

The South China Sea (SCS) is a semienclosed ocean basin and the largest marginal sea in Asia. The Asian monsoon is the most important factor influencing ocean circulation in the SCS (Wang et al., 2020). In summer, the SCS is affected by the southwest monsoon, which induces offshore Ekman transport and brings upwelling near the coast of southeast Vietnam (Xie et al., 2003, 2007; Li et al., 2014; Da et al., 2019; Ngo and Hsin, 2021). Additionally, the wind curl force of the southwest wind jet causes the double gyre circulation to form in the SCS with a northern cyclonic gyre and a southern anticyclonic gyre (Kuo et al., 2000; Metzger, 2003; Da et al., 2019; Ngo and Hsin, 2021). The cold coastal water is transported to the open SCS under the combined influence of the

southwest wind jet and southern anticyclonic gyre, forming a clear cold filament in the sea surface temperature (Li et al., 2017; Huang et al., 2020; Sun and Lan, 2021). Generally, the cold coastal water could spread eastward over most of the central SCS (approximately 115°E) in summer (Xie et al., 2003; Chen et al., 2021). The complex physical dynamic processes of the wind jet in the midwestern SCS attracted a lot of attention (Ning et al., 2004; Liu et al., 2012; Chen et al., 2014).

Biological processes in the marine ecosystem are substantially affected by physical processes such as eddies, upwelling, and oceanic fronts (Graham et al., 2001; Voynova et al., 2013; Duran-Campos et al., 2015; Liu et al., 2020). For instance, the upwelling delivers subsurface nutrients to the surrounding coastal ocean that supports phytoplankton primary production, and then zooplankton abundance also increases with phytoplankton (Voynova et al., 2013). In the midwestern SCS, many studies documented the physical-biological coupling influencing the chlorophyll-*a* (Chl *a*) concentration, demonstrating that the southwest wind jet and the anticyclonic eddy bring nutrient-rich water into the open SCS from the neritic region and thereby leading to an evident increase of Chl *a* (Wang and Tang, 2014; Zhao et al., 2018; Huang et al., 2020; Chen et al., 2021). Consequently, such an effect of physical-biological coupling is delivered to the zooplankton community. The rapid proliferation of phytoplankton generally leads to the increase of herbivorous zooplankton, thereby resulting in the change of zooplankton community structure (Voynova et al., 2013). Additionally, the intrusion of coastal water transports nearshore zooplankton to the open sea, which results in the change of zooplankton biodiversity (Pedersen et al., 2010). However, the mechanism of the influence of the wind-driven jet on zooplankton biodiversity and biomass in the midwestern SCS remains unclear.

Pelagic cnidarians are important taxa of marine zooplankton. As zooplanktivorous predators, medusae play an important role in the marine food web (Lynam et al., 2005; Purcell et al., 2007). Additionally, medusae compete with economic fishes and ingest fish eggs, larvae, and juveniles, causing a negative effect on the fishery resource replenishment (Purcell and Arai, 2001; Purcell and Sturdevant, 2001). The community structures and distributions of medusae are generally influenced by physical and hydrodynamic processes (Graham et al., 2001; Miglietta et al., 2008; Luo et al., 2014; Sevadjian et al., 2014; Kitajima et al., 2015). The distinct medusae taxa exhibit different reproductive modes and are distributed in different regions. For instance, meroplanktonic hydromedusae with a polyp stage mainly spread in the neritic areas, whereas holoplanktonic hydromedusae and siphonophores with no polyp stage are widely found in the neritic and the oceanic regions (Pavez et al., 2010). The increase of species number of meroplanktonic hydromedusae in the open sea indicates the invasion of coastal water (Pagès and Gili, 1992).

During September 9–17, 2011, we conducted an observational study in the midwestern SCS, to examine community structures and vertical distributions of medusae in the wind-driven jet (WJR) and non-wind-driven jet regions (NWJR). We aimed to study the effect of wind-driven jets on the zooplankton community from the perspective of the medusae. We addressed

two key questions with our study: (1) Does the coastal water transported by wind-driven jet affect the community structures and vertical distributions of medusae in the WJR? (2) How does the coastal water affect medusae in the WJR? These results significantly advance our understanding of the community structure of pelagic cnidarians in the midwestern SCS and highlight the role of coastal water intrusion in pelagic ecosystems in the open sea.

## MATERIALS AND METHODS

### Study Area

On September 9–17, 2011, a series of samples were obtained onboard R/V “Dong Fang Hong 2” in the midwestern SCS in three transects (nine stations, **Figure 1**). The transect A (TA) and C (TC) were located in the cyclonic and anticyclonic gyre areas (NWJR), respectively, while the transect B (TB) was located in the WJR.

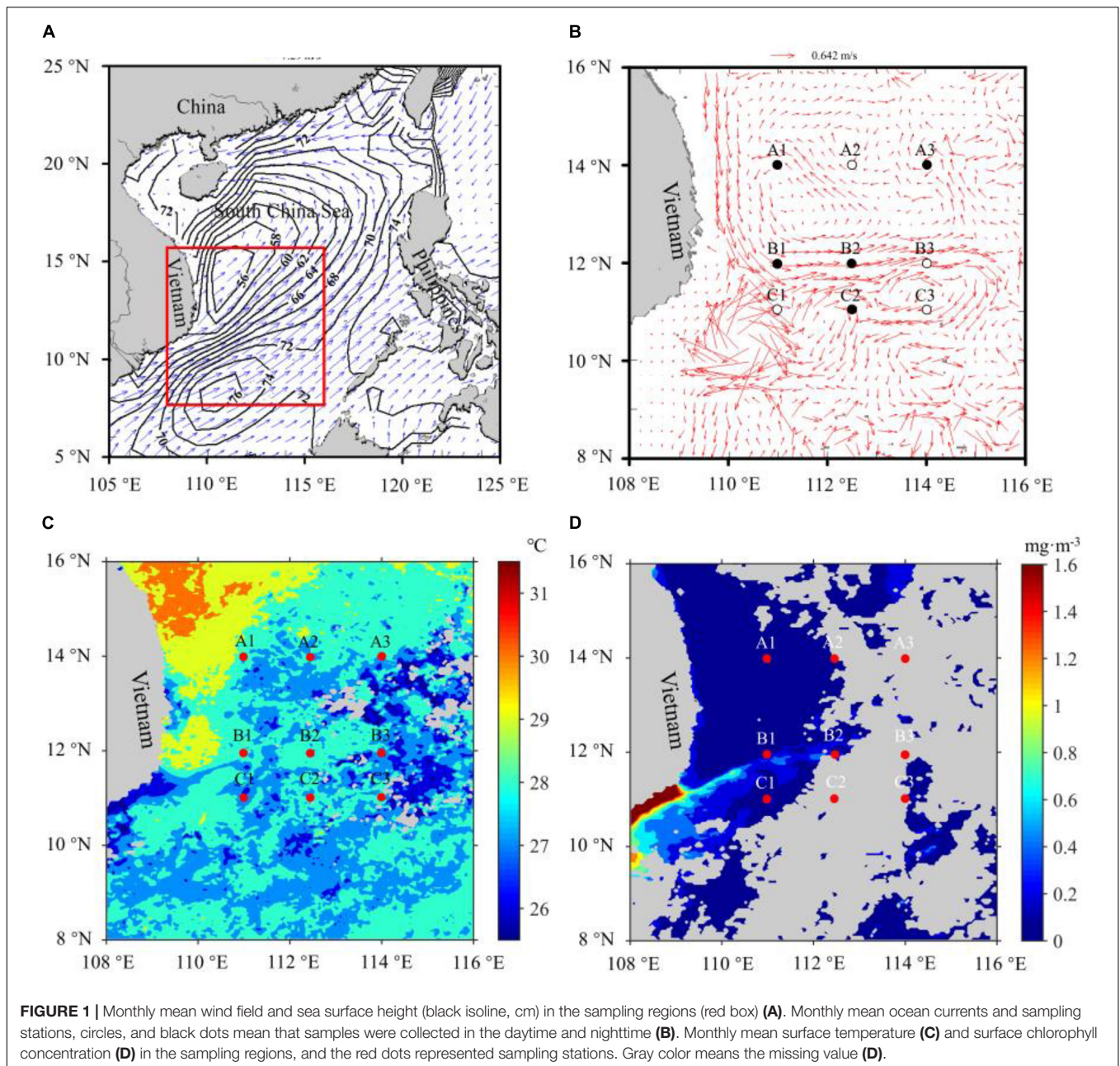
The data of surface currents, ocean wind field, and sea surface height during the investigation period were downloaded from the ECMWF (European Centre for Medium-Range Weather Forecasts, data source)<sup>1</sup>. Wind field and ocean surface currents showed that a strong southwest monsoon existed in the investigation region, and the double gyre circulation (cyclonic and anticyclonic gyres) formed in the SCS (**Figures 1A,B**). Sea surface height data also showed that convergence and divergence zones occurred in the southern and the northern SCS, respectively, and the height of the convergence center zone was 0.2 m higher than that of the divergence center zone (**Figure 1A**). The remotely sensed surface temperature and the chlorophyll concentration in SCS were obtained from Moderate Resolution Imaging Spectroradiometer level-3 products. Data presented a monthly average in September and a spatial resolution of around 4 km (data source)<sup>2</sup>. Surface temperature and the chlorophyll concentration data revealed that the wind-driven jet existed in the investigation region (**Figures 1C,D**).

### Sampling and Analysis

Zooplankton samples were collected from four strata (200–100, 100–50, 50–20, and 20–0 m), by using a Juday net with 0.5 m mouth diameter and 160  $\mu\text{m}$  mesh. The towing speed was 0.8–1  $\text{m}\cdot\text{s}^{-1}$ , and a flow meter was used to estimate the volume of filtered water. After each towing, zooplankton samples were preserved in 4% buffered formalin–seawater solution immediately. A total of 35 zooplankton samples were collected, and the sample of the 100–200 m layer at station B1 was not collected successfully. In the laboratory, samples were analyzed and counted under a stereomicroscope (Leica S8APO, Germany), and all hydromedusae and siphonophore were identified to the species level if possible. The wet weight biomass of the diet (zooplankton except for medusae) was measured using an analytical balance (SHPSI, JA2003N).

<sup>1</sup><http://apdrc.soest.hawaii.edu/>

<sup>2</sup><https://oceancolor.gsfc.nasa.gov/>



Temperature and salinity vertical profiles from the sea surface to 200 m depth were recorded using a conductivity–temperature–density (CTD) system (Sea-Bird SBE 911, United States). The seawater samples were collected at 0, 5, 25, 50, 75, 100, and 150 m depths for (Chl *a*) concentration measurement, and 0, 10, 25, 50, 75, 100, and 200 m depth for nutrient concentration measurement. Chl *a* samples were filtered through the Merck Isopore filter with a diameter of 25 mm and a pore size of 0.4  $\mu\text{m}$  and frozen in the liquid nitrogen for further analysis. The nutrients samples were filtered through precombusted (460°C for 6 h) 0.7  $\mu\text{m}$  Whatman GF/F filters and collected in polyethylene bottles at  $-20^{\circ}\text{C}$  for laboratory analysis. A pH meter (DELTA320, Switzerland) was used to measure the pH. In the laboratory,

Chl samples were extracted in 90% acetone for 24 h in the dark and measured using the Shimadzu Design 20A Liquid Chromatograph (SHIMADZU, Japan). Nutrient concentrations including phosphate, silicate, and dissolved inorganic nitrogen (DIN, nitrate + nitrite + ammonium), were measured by continuous flow autoanalyzer systems (AAIII) according to standard colorimetric techniques (Grasshoff et al., 1983). Dissolved oxygen (DO) concentration was evaluated *via* the Winkler titration method (Wilkin et al., 2001).

## Data Analysis

The abundance of medusae was standardized to individuals per  $\text{m}^{-3}$ . Each species of hydromedusae, as well as a siphonophore,

was ranked in accordance with the abundance, and the top three species were selected as dominant species. The abundance of medusae was arranged in descending order to obtain the K-dominance curve (Clarke, 1993).

Multivariate analyses were conducted using the PRIMER software version 6 (PRIMER-E, United Kingdom). The abundance data of medusae were subjected to the  $\log(x + 1)$  transformation and used to build a similarity matrix between stations based on the Bray–Curtis coefficient of similarity (Field et al., 1982). Station interrelations were clustered based on the average linkage group classification (Field et al., 1982). The analysis of similarity (ANOSIM) was used to determine whether clusters were significantly different (Clarke, 1993). In pairwise comparisons, an *R*-statistic value close to 1 indicated a considerable difference. The similarity percentages (SIMPER) procedure (Clarke, 1993) was used to identify which species contributed to cluster differences. The correlation between the zooplankton abundance and environmental factors was analyzed using the RELATE function. The generalized additive model (GAM) was used to identify relationships between the abundance of medusae and environment factors through the “gam” function in the R package mgcv (Wood, 2006). The best model was selected based on minimizing the generalized cross-validation (GCV) criterion that measures the degree of penalization during fitting (Wood, 2006). Environmental factors included temperature, salinity, Chl *a* concentration, and wet weighted biomass of diet (labeled as “diet” in this study). The medusae abundance, Chl *a* concentration, and diet were subjected to  $\log_{10}$  transformations before the analysis (Campbell, 1995).

One-way ANOVA was used to determine the dissimilarity of zooplankton (hydromedusae, siphonophore, and wet weight diet) in different regions; SPSS 25 (IBM, United States) was used to analyze this. The Kolmogorov–Smirnov test was used to determine the normality of the zooplankton abundance before ANOVA.

## RESULTS

### Environmental Factors

The changing vertical structure of the water column among TA, TB, and TC was clearly indicated by the CTD profiles (Figure 2). The thermocline depth and strength among TA, TB, and TC were remarkably different. A weak and shallow thermocline of TA, which is located in the cyclonic gyre area, was detected at approximately 20 m. Strong thermoclines were recorded both in TB and TC, while the thermocline in TC (60 m), which is located in the anticyclonic gyre area, was deeper than that in TB (50 m). The surface salinity of TB was significantly lower than that of TA, suggesting that the low-salinity water in the coastal region was carried to the WJR by the southwest wind jet and the anticyclonic gyre. Additionally, low salinity was also characteristic of the surface water of TC, which indicated that the TC was influenced by the coastal water.

The vertical distributions of Chl *a* concentration among three transects were substantially different (Figure 3A). The maximum Chl *a* concentration in TA and TC were observed at 50 and 75 m,

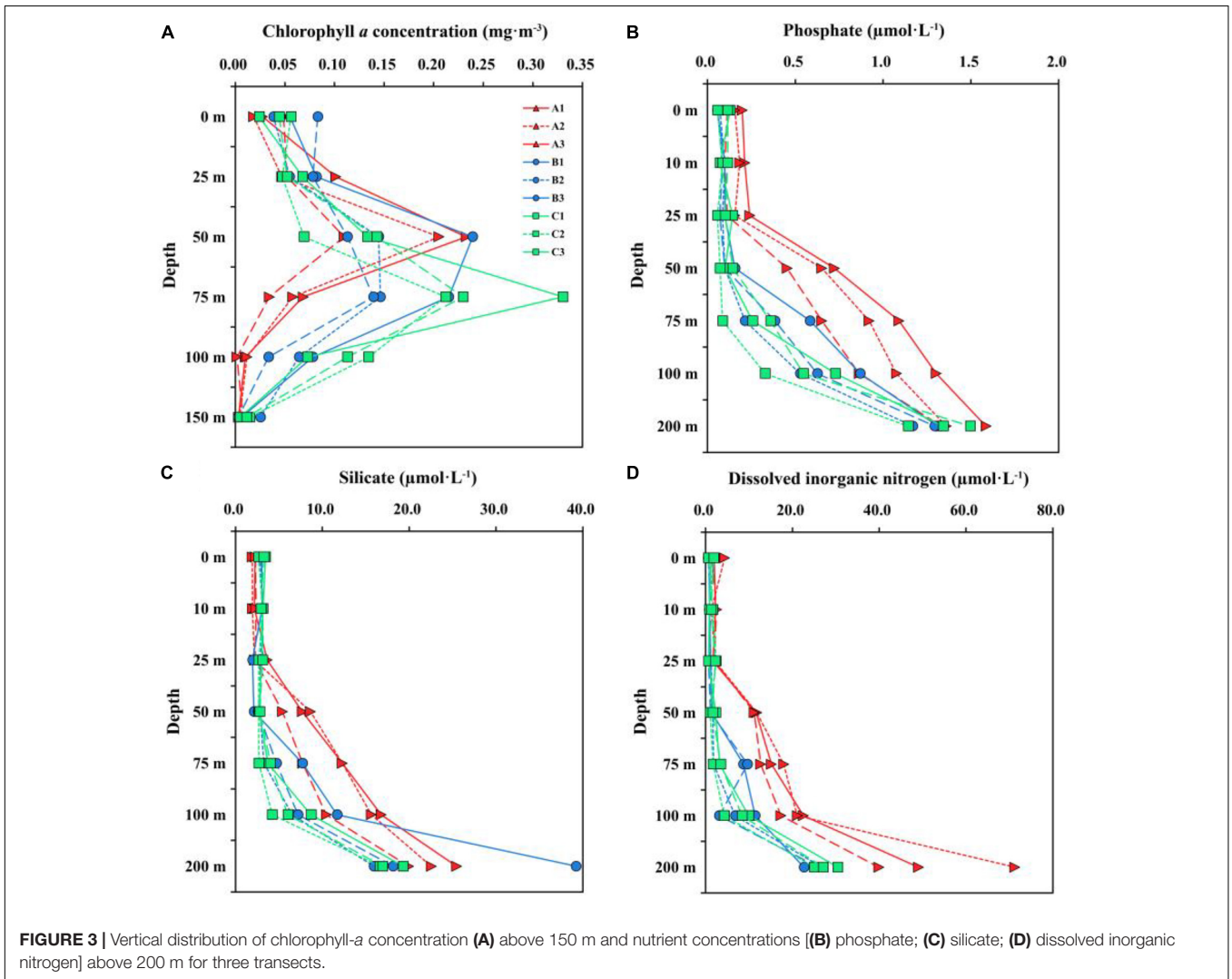
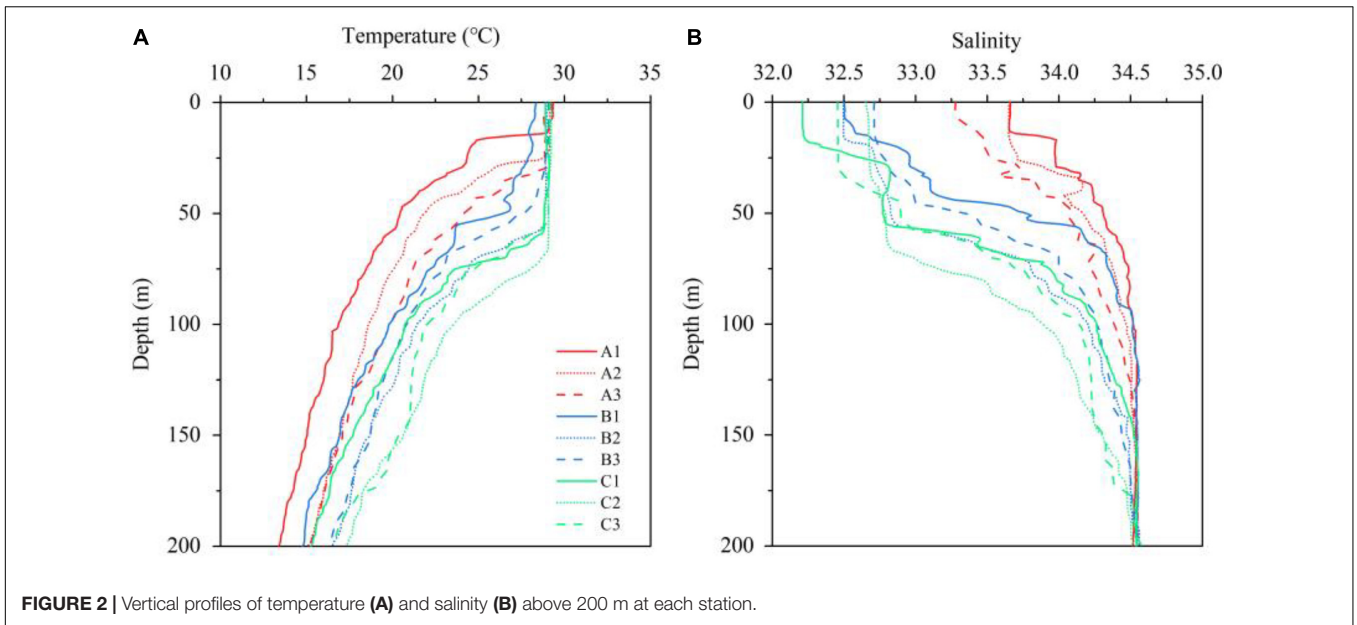
respectively, while TB had high Chl *a* concentration at both 50 and 75 m depths. The surface Chl *a* concentration in TA, TB and TC were  $0.03 \pm 0.02$ ,  $0.06 \pm 0.02$ , and  $0.04 \pm 0.02$   $\text{mg}\cdot\text{m}^{-3}$ , respectively. Additionally, the Chl *a* concentration at station B1 was high than those at station B2 and B3, indicating that nutrients may be gradually consumed during the eastward flow of coastal water. The vertical distributions of nutrient concentrations, DO concentration and pH were remarkably different in three transects, and these factors in TB were similar to that in TC compared to TA (Figure 3 and Supplementary Figure 1). The nutrient concentrations (except surface silicate concentration) and DO concentration in TA were higher than those in the TB and TC, whereas the pH was high in TB and TC.

### Species Composition and Community Structure of Medusae

A total of 49 hydromedusae species was recorded in TB, which was higher than that in TA and TC (32 and 33 species, respectively; Supplementary Table 1). The species number of holoplanktonic hydromedusae (Subclass Narcomedusae and Trachymedusae) in TB (18 species) were similar to that in TA and TC (17 and 15 species, respectively; Figure 4 and Supplementary Table 1), whereas the species number of meroplanktonic hydromedusae (Subclass Anthomedusae and Leptomedusae) in TB (31 species) were approximately twice that of the TA and TC (15 and 18 species, respectively; Figure 4), suggesting that coastal meroplanktonic hydromedusae were carried by the wind-driven jet to the WJR. A total of 31 siphonophore species in TB were detected and this finding was similar to that in TB and TC (30 and 30 species; Figure 4). Additionally, the species number of hydromedusae and siphonophore showed significant differences in different layers among the three transects (Supplementary Table 1). The results of the K-dominance curves showed that the richness of meroplanktonic hydromedusae in TB was higher than that in TA and TC, while the evenness of meroplanktonic hydromedusae was high in TA, followed by TB and TC (Figure 4).

The mean total abundance of holoplanktonic hydromedusae in TB ( $38.2 \pm 9.3$   $\text{ind}\cdot\text{m}^{-3}$ ) was significantly higher than those in TA ( $13.4 \pm 1.6$   $\text{ind}\cdot\text{m}^{-3}$ ; one-way ANOVA,  $p = 0.002$ ) and TC ( $12.8 \pm 2.7$   $\text{ind}\cdot\text{m}^{-3}$ ;  $p = 0.002$ ), while siphonophore in TB ( $26.6 \pm 8$   $\text{ind}\cdot\text{m}^{-3}$ ) was high but not significantly different with that in TA ( $18.2 \pm 5.8$   $\text{ind}\cdot\text{m}^{-3}$ ;  $p = 0.165$ ) and TC ( $25.2 \pm 5.3$   $\text{ind}\cdot\text{m}^{-3}$ ;  $p = 0.809$ ). However, the highest total abundance of meroplanktonic hydromedusae was recorded in TC ( $4.8 \pm 1.1$   $\text{ind}\cdot\text{m}^{-3}$ ), followed by the TB ( $3 \pm 1.5$   $\text{ind}\cdot\text{m}^{-3}$ ) and TA ( $0.8 \pm 0.1$   $\text{ind}\cdot\text{m}^{-3}$ ; Table 1).

The vertical distributions of hydromedusae and siphonophore among the three transects were evidently different (Table 1 and Figure 5). The maximum abundances of hydromedusae and siphonophore in TA and TC were recorded at the 20–50 m layer, except for meroplanktonic hydromedusae in TA where the maximum abundance was detected at the 0–20 m strata. However, the maximum abundances of the hydromedusae and siphonophore in TB were documented at the 0–20 m layer. Medusae at three transects were mainly distributed above the



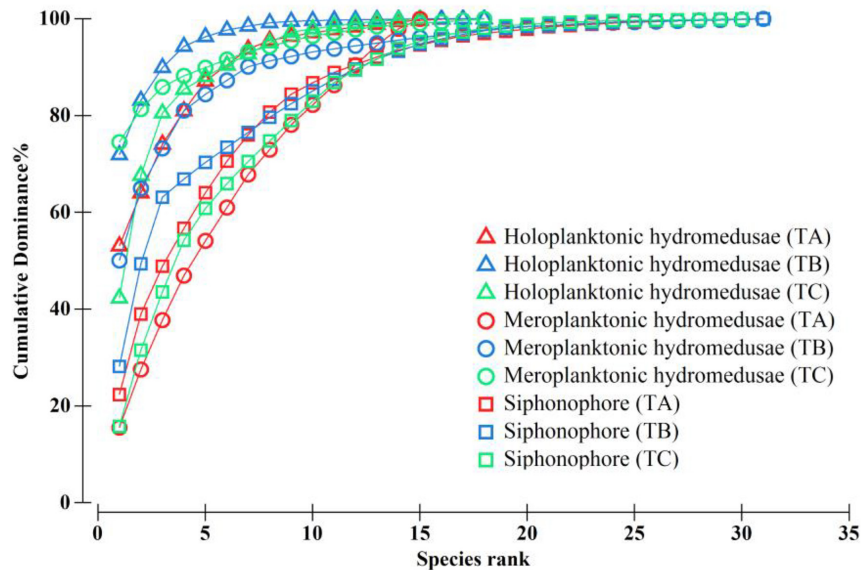


**FIGURE 4** | K-dominance curves of different groups of medusae in the wind-driven jet (WJR) and the non-wind-driven jet (NWJR). TA–TC represented transect A, B, and C, respectively.

thermocline and showed no remarkable diel vertical migration (Figures 2, 5). Thus, the vertical distribution of medusae was remarkably influenced by the thermocline in three transects. Additionally, the abundance of medusae above the thermocline in TB was higher than that in TA and TC, whereas their abundance below the thermocline was similar among TA, TB, and TC (Figure 5), indicating that the coastal water only affected the abundance of medusae above the thermocline in TB.

The diet zooplankton abundance and wet biomass existed remarkable differences among the three transects (Supplementary Table 1). The total abundance of diet zooplankton in TA, TB, and TC were  $1030.2 \pm 279.4$ ,  $2946.6 \pm 1776.2$ , and  $2270.9 \pm 446.8$  ind·m<sup>-3</sup>, respectively. Copepods were the dominant group in each layer of three transects (Supplementary Figure 2). Additionally, total wet biomass of the diet zooplankton in TA, TB, and TC were  $228.8 \pm 92.8$ ,  $405.1 \pm 171.3$ , and  $263.6 \pm 81.0$  w/w mg·m<sup>-3</sup>, respectively. The vertical distribution of mean wet weight biomass of diet was similar among three transects, which decreased along with increasing depth (Table 1 and Figure 5).

*Aglaura hemistoma*, *Amphogona apsteini*, *Cunina peregrina*, *Eirene hexanemalis*, *Liriope tetraphylla*, *Rhopalonema velatum*, *Sminthea eurygaster*, and *Solmundella bitentaculata* were the dominant species of hydromedusae, and *A. hemistoma* was the most important species in three transects (Table 2). Except for *E. hexanemalis*, other dominant species belong to holoplanktonic hydromedusae. Additionally, the dominant species of hydromedusae among the three transects were evidently different (Table 2). *A. apsteini* was the dominant species in TA, whereas *S. bitentaculata*, as the dominant species, only appeared in TB. Similar to hydromedusae, the dominant species of siphonophore among three transects also existed remarkable differences. *Abylopsis eschscholtzi* and *Sulculeolaria chuni*, as the

dominant species, only appeared in TA, while *Bassia bassensis* and *Eudoxoides mitra* were the dominant species in TC (Table 2).

Cluster analyses indicated that the medusae community above the thermocline was evidently different from the community in the deeper layers in three transects (Supplementary Figure 3). The dominant species in the three transects were significantly different among each layer (Table 2). *A. hemistoma* was the most dominant species of hydromedusae at the 0–20, 20–50, and 50–100 m layers in TA, whereas *S. eurygaster* had the highest abundance at the 100–200 m layer. *A. hemistoma* was the most dominant species of hydromedusae at each layer in TB, but its abundance decreased with increasing depth. *E. hexanemalis* and *L. tetraphylla* had the highest abundance at the 0–20 and 50–100 m layers in TC, respectively, whereas *A. hemistoma* was the most dominant species at the 20–50 and 100–200 m layers. As for siphonophore, *C. appendiculata* and *E. spiralis* were the most dominant species of siphonophore at the 0–20 and 20–50 m layers, respectively, in TA, whereas *Lensia subtilis* had the highest value at the 50–100 and 100–200 m layers. In TB, *Lensia subtiloides* and *L. subtilis* had the highest value at 0–20 and 100–200 m layers, whereas *Diphyes chamissonis* was the most dominant species at the 20–50 and 50–100 m layers. *L. subtiloides* had the highest value at the 0–20 and 20–50 m layers in TC, while *L. subtilis* was the most dominant species at the 50–100 and 100–200 m layers.

## Correlation Analyses Between Medusae and Environmental Factors

The RELATE analyses showed that medusae were significantly correlated with environmental factors ( $r = 0.667$ ,  $p < 0.001$ ). The generalized additive model (GAM) analyses showed the relationship between medusae and environmental variables,

**TABLE 1** | Vertical distribution of holoplanktonic hydromedusae (HH), meroplanktonic hydromedusae (MH) siphonophore (SI), and diet zooplankton in three transects.

Layer	Transect A					Transect B					Transect C				
	Mean abundance (ind.m <sup>-3</sup> )					Mean abundance (ind.m <sup>-3</sup> )					Mean abundance (ind.m <sup>-3</sup> )				
	HH	MH	SI	Diet	biomass (WW mg.m <sup>-3</sup> )	HH	MH	SI	Diet	biomass (WW mg.m <sup>-3</sup> )	HH	MH	SI	Diet	biomass (WW mg.m <sup>-3</sup> )
0-20 m	3.9 ± 1.5	0.3 ± 0.3	5.8 ± 3.2	292.7 ± 189.8	91.1 ± 36.8	21.8 ± 7.8	1.4 ± 0.7	7.8 ± 1.5	1202.3 ± 329.7	146.3 ± 68.5	2.2 ± 0.9	1.7 ± 0.6	6.9 ± 2.7	1455.6 ± 758.6	95.9 ± 51.9
20-50 m	5.3 ± 1.1	0.2 ± 0.3	6.6 ± 0.9	538.4 ± 182.5	80.8 ± 43.6	8.5 ± 6.7	0.8 ± 1.0	7.3 ± 4.7	897.6 ± 1200.0	112.3 ± 49.1	5.3 ± 2.6	2.5 ± 0.5	9.6 ± 4.9	439.2 ± 329.0	81.0 ± 34.1
50-100 m	3.2 ± 0.8	0.2 ± 0.2	4.1 ± 1.5	164.1 ± 57.8	43.1 ± 14.1	5.6 ± 2.4	0.5 ± 0.1	6.7 ± 1.9	503.7 ± 285.7	87.3 ± 40.5	3.7 ± 0.6	0.4 ± 0.1	6.11 ± 0.5	218.2 ± 260.5	58.9 ± 11.1
100-200 m	1.0 ± 0.6	0.1 ± 0.1	1.8 ± 1.2	35.0 ± 19.5	13.8 ± 4.3	2.3 ± 1.9	0.3 ± 0.1	4.8 ± 3.6	342.9 ± 227.0	59.2 ± 45.7	1.7 ± 0.1	0.2 ± 0.05	2.7 ± 1.7	157.8 ± 157.0	27.8 ± 6.1
Total	13.4 ± 1.6	0.8 ± 0.1	18.2 ± 5.8	1030.2 ± 279.4	228.8 ± 92.8	38.2 ± 9.3	3.0 ± 1.5	26.6 ± 8.0	2946.6 ± 1776.2	405.1 ± 171.3	12.8 ± 2.7	4.8 ± 1.1	25.2 ± 5.3	2270.9 ± 446.8	263.6 ± 81.0

such as temperature, salinity, Chl *a*, and diet (Table 3 and Figure 6). The holoplanktonic hydromedusae and siphonophore abundances were mainly affected by the diet ( $p = 0.009$  and  $p < 0.001$ , respectively), and these abundances increased with the increasing diet (Figures 6a4,c4). Meroplanktonic hydromedusae were influenced by the combination of temperature, salinity, and diet, which abundance decreased with the increasing temperature and salinity (Figures 6b1,b2,b4). Moreover, the abundance of meroplanktonic hydromedusae increased with the increasing diet when the diet was low, but it no longer increased when the diet was abundant. Additionally, the dominant species were influenced by different environmental factors (Table 3). *A. hemistoma*, as the most abundant species, had a strong correlation with diet ( $p < 0.001$ ), while *E. hexanemalis*, which belonged to meroplanktonic hydromedusae, was affected by the combination of temperature and diet ( $p = 0.014$  and  $p = 0.037$ , respectively). As the dominant species of siphonophore, *A. eschscholtzi* ( $p = 0.015$ ), *Abylopsis tetragona* ( $p = 0.009$ ), *D. chamissonis* ( $p = 0.044$ ), *L. subtilis* ( $p = 0.004$ ) and *L. subtiloides* ( $p = 0.004$ ) was mainly influenced by the diet.

## DISCUSSION

This study suggested that an evident intrusion of the wind-driven jet was detected in the midwestern SCS (Figure 1), and the abundances of medusae and its diet organisms were remarkably higher in the WJR than that in the NWJR (Figure 5 and Table 1). However, the Chl *a* concentration showed no significant difference between the WJR and NWJR (Figure 3A), the nutrient concentration was lower in the WJR than that in the NWJR (Figures 3B-D). The nutrient in upwelling regions in Vietnam was replete (Ke et al., 2012; Lu et al., 2018), but the nutrient of coastal upwelling water by the process of horizontal transport was gradually consumed by phytoplankton and diluted by the surrounding waters. The WJR in this study was located at the end of the wind-driven jet and the nutrient was getting limited as the wind-driven jet moved offshore which slows the growth of phytoplankton. Moreover, a low nutrient at the end of the wind-driven jet is also caused by the absence of deep nutrient supplementation due to the strongly stratified waters (Figure 2). When the phytoplankton growth slows, the zooplankton grazers begin to “catch up,” and their top-down control causes the further decline in phytoplankton biomass. The growth of zooplankton lags behind the growth of phytoplankton and nutrient supply is commonly observed in marine ecosystems such as upwelling and bloom (Voynova et al., 2013; George et al., 2015). Our results in concert with previous studies suggested the unsynchronized changes of hydrological, chemical, and biological characteristics. Furthermore, the increased diet substantially promoted the increase of medusae abundance, which indicated that medusae were under the bottom-up control of their prey. It indicated that physical processes drove the combination of bottom-up and top-down control in this ecosystem. Additionally, the lagging biological characteristic can be the amplification, or echo of the physico-chemical signal of the ocean, reflecting and backtracking the evolution of environmental conditions.

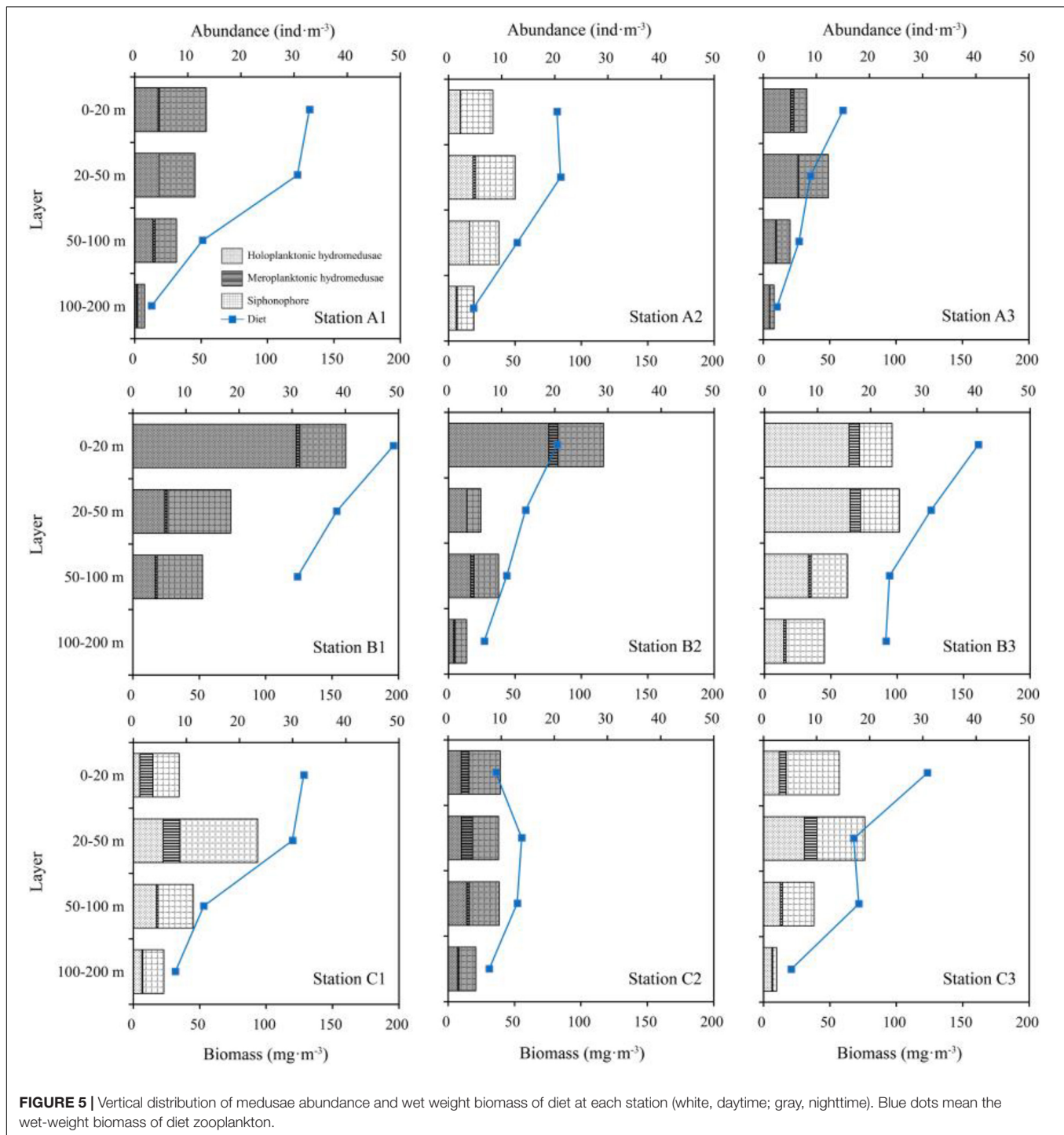


**FIGURE 5** | Vertical distribution of medusae abundance and wet weight biomass of diet at each station (white, daytime; gray, nighttime). Blue dots mean the wet-weight biomass of diet zooplankton.

Generally, many physical processes such as ocean fronts and upwelling could drive primary production and fishery production (Aristegui et al., 2009; Woodson and Litvin, 2015). However, medusae are predators with a broad zooplanktivorous diet (Lynam et al., 2005; Purcell et al., 2007), and they could exert substantial pressure on prey organisms (Kideys and Romanova, 2001). The rapid growth of medusae potentially allows them to outcompete planktivorous fish species (Brodeur et al., 2008).

Additionally, medusae ingest fish eggs, larvae, and juveniles, causing a negative effect on fishery resource replenishment (Purcell and Arai, 2001). Thus, in this study, the abundance of medusae in the WJR increased substantially, which may play a negative role in fishery production.

The species composition and the abundance distribution of medusae in the WJR were significantly influenced by the intrusion of wind-driven jets (**Supplementary Table 1** and

**TABLE 2** | Mean abundance of dominant species at each layer for three transects.

Species	Mean abundance (ind·m <sup>-3</sup> )											
	Transect A				Transect B				Transect C			
	0–20 m	20–50 m	50–100 m	100–200 m	0–20 m	20–50 m	50–100 m	100–200 m	0–20 m	20–50 m	50–100 m	100–200 m
<i>Aglaura hemistoma</i> <sup>h</sup>	<b>3.3 ± 1.2</b>	<b>2.5 ± 0.8</b>	<b>1.2 ± 0.7</b>	<b>0.1 ± 0.1</b>	<b>18.8 ± 9.4</b>	<b>5.1 ± 3.1</b>	<b>2.5 ± 1.6</b>	<b>0.8 ± 0.7</b>	<b>1.0 ± 0.5</b>	<b>2.9 ± 2.2</b>	<b>1.2 ± 0.7</b>	<b>0.4 ± 0.1</b>
<i>Amphogona apicata</i> <sup>h</sup>	–	–	–	<b>0.1 ± 0.1</b>	–	–	–	0.02 ± 0.03	0.3 ± 0.4	–	–	0.1 ± 0.1
<i>Cunina peregrina</i> <sup>h</sup>	<b>0.1 ± 0.2</b>	<b>0.8 ± 1.4</b>	<b>0.4 ± 0.5</b>	0.02 ± 0.03	0.8 ± 1.1	<b>2.3 ± 3.2</b>	<b>1.0 ± 1.5</b>	<b>0.2 ± 0.3</b>	–	0.2 ± 0.3	0.1 ± 0.1	0.03 ± 0.1
<i>Eirene hexanemalis</i> <sup>m</sup>	–	0.1 ± 0.1	–	–	0.7 ± 0.3	<b>0.6 ± 0.9</b>	0.2 ± 0.1	0.02 ± 0.03	<b>1.2 ± 0.7</b>	<b>2.1 ± 0.5</b>	0.3 ± 0.1	0.02 ± 0.03
<i>Liriope tetraphylla</i> <sup>h</sup>	<b>0.3 ± 0.2</b>	0.4 ± 0.3	0.1 ± 0.1	0.02 ± 0.03	<b>0.9 ± 0.5</b>	0.4 ± 0.1	<b>1.2 ± 1.0</b>	0.1 ± 0.1	<b>0.6 ± 0.6</b>	<b>1.1 ± 0.1</b>	<b>1.5 ± 0.1</b>	0.2 ± 0.2
<i>Rhopalonema velatum</i> <sup>h</sup>	0.08 ± 0.1	<b>0.6 ± 0.2</b>	<b>0.7 ± 0.6</b>	0.07 ± 0.06	0.08 ± 0.1	0.3 ± 0.3	0.4 ± 0.4	0.02 ± 0.03	0.08 ± 0.1	0.6 ± 0.4	<b>0.7 ± 0.8</b>	<b>0.3 ± 0.2</b>
<i>Sminthea eurygaster</i> <sup>h</sup>	–	–	0.1 ± 0.1	<b>0.3 ± 0.3</b>	–	–	0.2 ± 0.2	<b>0.4 ± 0.04</b>	–	–	0.03 ± 0.1	<b>0.3 ± 0.05</b>
<i>Solmundella bitentaculata</i> <sup>h</sup>	–	0.3 ± 0.2	0.1 ± 0.1	0.06 ± 0.08	<b>1.1 ± 0.7</b>	0.4 ± 0.5	0.2 ± 0.1	–	0.3 ± 0.2	0.3 ± 0.3	–	0.1 ± 0.1
<i>Abylopsis eschscholtzi</i> <sup>s</sup>	0.04 ± 0.07	0.6 ± 0.6	<b>0.7 ± 0.4</b>	0.04 ± 0.01	0.1 ± 0.1	–	0.2 ± 0.1	0.1 ± 0.1	0.3 ± 0.1	0.6 ± 0.3	0.2 ± 0.1	0.2 ± 0.2
<i>Abylopsis tetragona</i> <sup>s</sup>	–	<b>1.3 ± 0.9</b>	0.5 ± 0.2	0.1 ± 0.1	–	0.1 ± 0.2	0.5 ± 0.1	0.4 ± 0.3	–	0.3 ± 0.3	0.4 ± 0.3	<b>0.3 ± 0.3</b>
<i>Bassia bassensis</i> <sup>s</sup>	–	0.3 ± 0.05	–	–	0.4 ± 0.5	0.1 ± 0.1	0.04 ± 0.1	–	<b>1.0 ± 0.2</b>	1.1 ± 0.4	<b>0.6 ± 0.4</b>	0.03 ± 0.03
<i>Chelophyes appendiculata</i> <sup>s</sup>	<b>3.0 ± 2.5</b>	0.4 ± 0.7	<b>0.6 ± 0.4</b>	0.1 ± 0.1	<b>0.7 ± 0.9</b>	0.1 ± 0.2	0.1 ± 0.1	0.05 ± 0.06	<b>2.0 ± 2.0</b>	<b>1.6 ± 0.6</b>	0.3 ± 0.1	0.1 ± 0.1
<i>Diphyes chamissonis</i> <sup>s</sup>	<b>0.5 ± 0.2</b>	0.6 ± 1.0	0.1 ± 0.1	–	<b>2.2 ± 3.0</b>	<b>3.0 ± 3.4</b>	<b>1.7 ± 2.3</b>	0.05 ± 0.001	0.2 ± 0.3	<b>1.4 ± 1.4</b>	0.1 ± 0.1	0.04 ± 0.05
<i>Eudoxoides mitra</i> <sup>s</sup>	0.2 ± 0.3	0.1 ± 0.2	0.02 ± 0.03	0.1 ± 0.2	0.1 ± 0.1	0.2 ± 0.2	0.4 ± 0.3	0.3 ± 0.2	–	0.2 ± 0.4	<b>0.7 ± 0.4</b>	0.1 ± 0.1
<i>Eudoxoides spiralis</i> <sup>s</sup>	–	<b>1.3 ± 0.3</b>	0.05 ± 0.1	0.03 ± 0.03	0.03 ± 0.05	0.1 ± 0.1	0.4 ± 0.2	<b>0.5 ± 0.6</b>	–	–	0.5 ± 0.1	0.2 ± 0.2
<i>Lensia meteoris</i> <sup>s</sup>	–	–	0.2 ± 0.1	<b>0.2 ± 0.2</b>	–	–	0.3 ± 0.3	<b>0.6 ± 0.1</b>	–	–	0.1 ± 0.1	<b>0.2 ± 0.2</b>
<i>Lensia subtilis</i> <sup>s</sup>	0.1 ± 0.1	<b>0.7 ± 0.5</b>	<b>1.3 ± 1.0</b>	<b>0.9 ± 0.5</b>	–	<b>0.7 ± 0.6</b>	<b>1.4 ± 0.7</b>	<b>1.9 ± 1.1</b>	0.1 ± 0.1	0.4 ± 0.8	<b>1.5 ± 0.6</b>	<b>1.0 ± 0.6</b>
<i>Lensia subtiloides</i> <sup>s</sup>	0.4 ± 0.1	0.1 ± 0.1	0.1 ± 0.1	<b>0.1 ± 0.1</b>	<b>2.8 ± 0.7</b>	<b>1.8 ± 1.8</b>	<b>0.6 ± 0.7</b>	0.2 ± 0.3	<b>2.1 ± 0.4</b>	<b>1.8 ± 1.3</b>	0.1 ± 0.1	0.04 ± 0.001
<i>Sulculeolaria chuni</i> <sup>s</sup>	<b>0.7 ± 0.7</b>	0.2 ± 0.3	0.1 ± 0.03	0.02 ± 0.03	0.4 ± 0.3	0.1 ± 0.1	0.1 ± 0.1	0.1 ± 0.1	–	0.3 ± 0.3	0.2	0.04 ± 0.05

The bold font style indicates that the species was the dominant species in the layer. “–” represents that the species has not appeared in this layer. h, holoplanktonic hydromedusae; m, meroplanktonic hydromedusae; s, siphonophore.

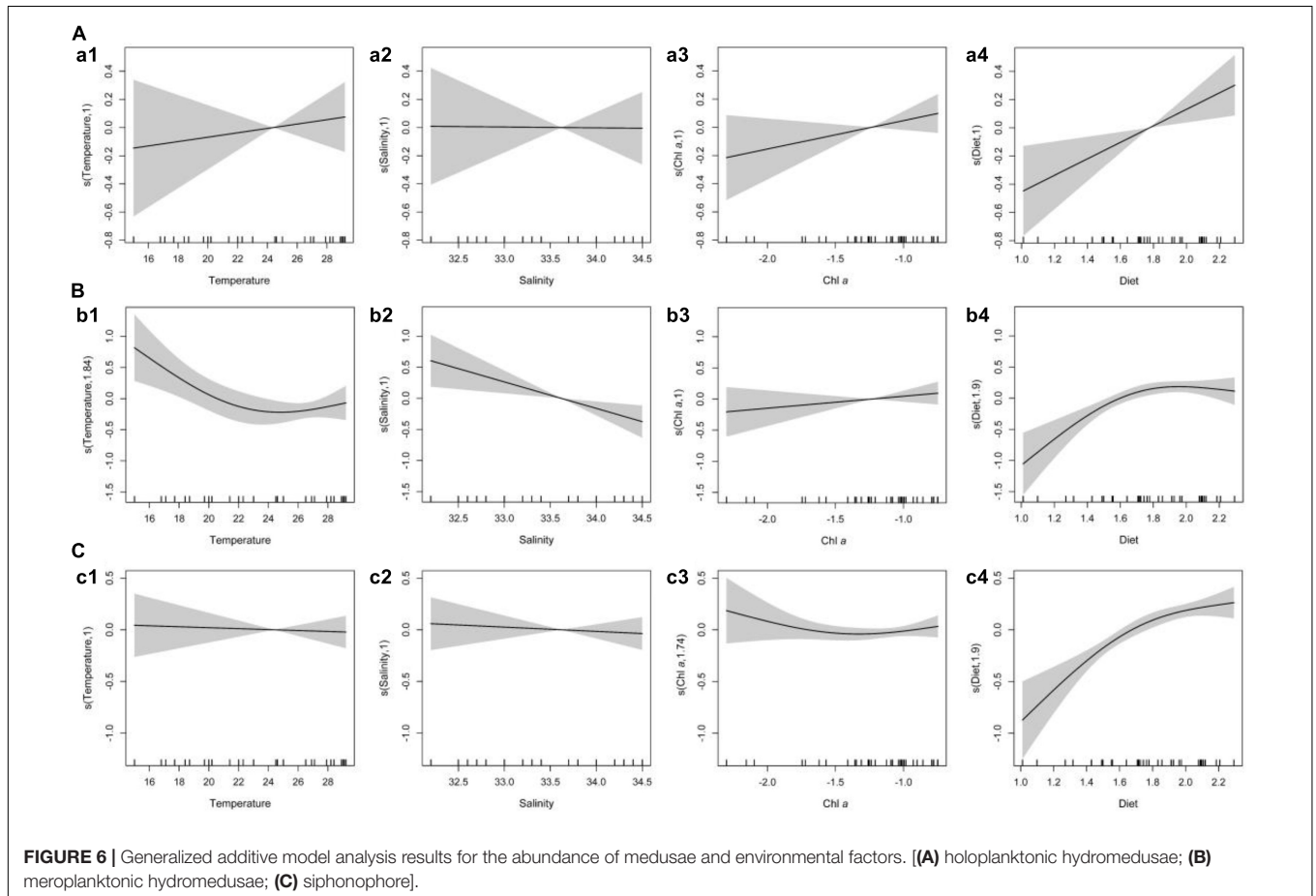
**Figure 7**). In terms of species number, the medusae in the WJR were higher than that in the NWJR due to the influence of the coastal water intrusion. Similar conditions were also recorded in other marine ecosystems (Lučić et al., 2009). Additionally, the species numbers of different taxa were affected differently by the wind-driven jet. The species number of meroplanktonic hydromedusae (Anthomedusae and Leptomedusae) in the WJR was higher than that in the NWJR, whereas the species numbers of holoplanktonic hydromedusae and siphonophore were similar between the WJR and the NWJR (**Supplementary Table 1**). Anthomedusae and Leptomedusae are mostly meroplanktonic with a polyp stage, which needs to be anchored to the bottom of neritic areas (Pavez et al., 2010). Rodriguez et al. (2017) suggested that meroplanktonic medusae contributed more to the neritic communities, and they were more restricted in

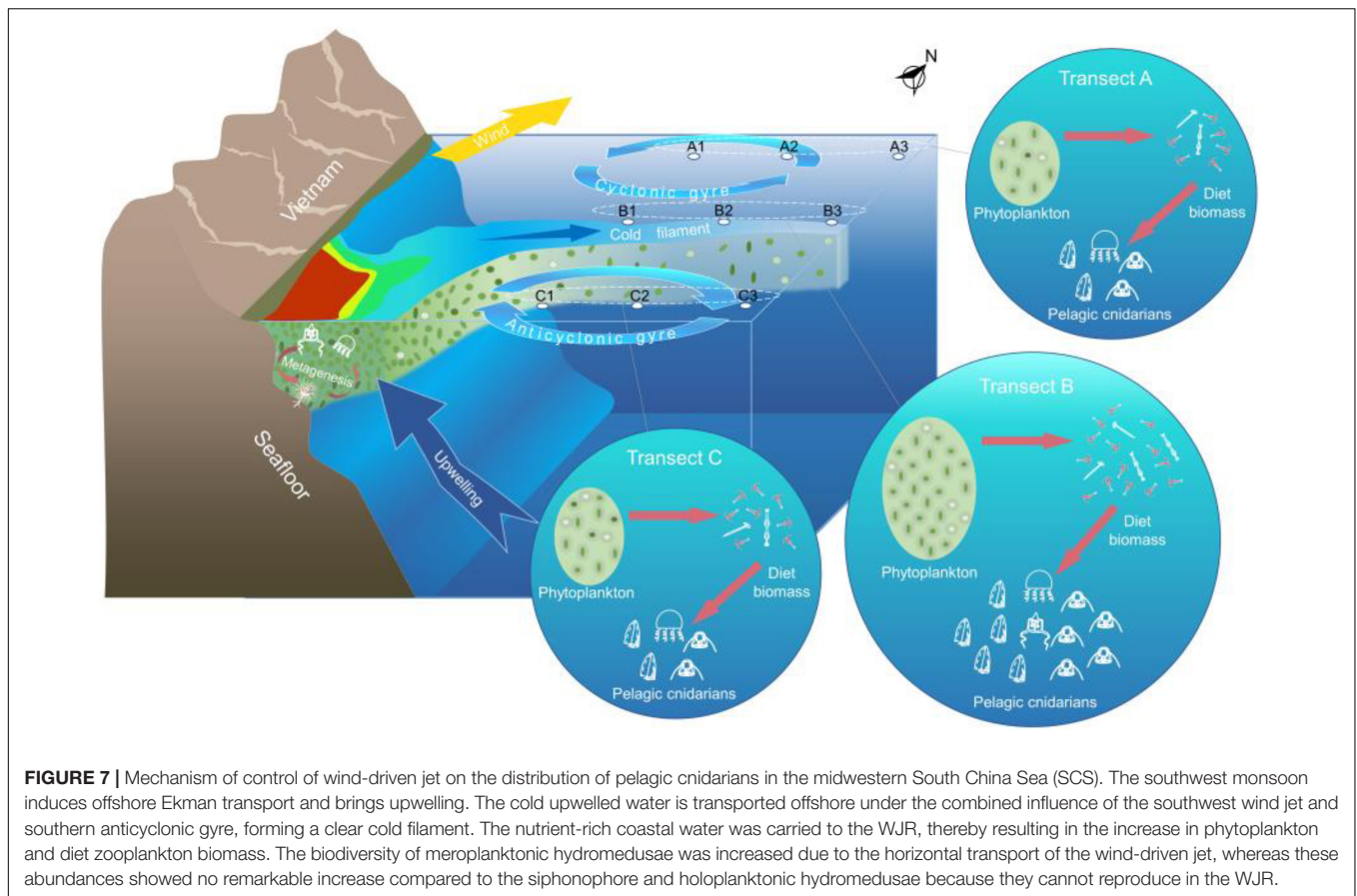
distribution than holoplanktonic ones. The wind-driven jet in the southern SCS transported the coastal water containing abundant meroplanktonic hydromedusae species to the WJR, thereby increasing the species number of meroplanktonic hydromedusae (**Figure 7**). The lifespan of meroplanktonic hydromedusae varies between a few hours to a few years, but most species have a lifespan of more than 2 months (Brock and Strehler, 1963; Roosen-Runge, 1970; Mills, 1993). The velocity of the southwest wind jet was 30–110 cm·s<sup>-1</sup> (Fang et al., 1997; Chen et al., 2012; Li et al., 2017; Da et al., 2019), and it will take a maximum of about 3 weeks for the coastal water transported to the farthest station (B3, 550 km off the coastline) in this study. The meroplanktonic hydromedusae can be carried to the WJR by horizontal transport considering the longevity of jellyfish and the age of water. Nevertheless, holoplanktonic hydromedusae and siphonophores

**TABLE 3** | Generalized additive model results for medusae and environmental factors among three transects.

Taxa	P-value				R <sup>2</sup>	GCV
	Temperature	Salinity	Chl a	Diet		
Holoplanktonic hydromedusae	0.552	0.967	0.164	0.009**	0.508	0.087
Meroplanktonic hydromedusae	0.016*	0.007**	0.308	<0.001***	0.749	0.069
Siphonophore	0.780	0.649	0.353	<0.001***	0.702	0.032
<i>Aglaura hemistoma</i> <sup>h</sup>	0.220	0.394	0.165	<0.001***	0.603	0.139
<i>Amphogona apicata</i> <sup>h</sup>	0.315	0.873	0.128	0.080	0.370	0.114
<i>Cunina peregrina</i> <sup>h</sup>	0.129	0.525	0.384	0.174	0.096	0.199
<i>Liriope tetraphylla</i> <sup>h</sup>	0.792	0.062	0.143	0.306	0.205	0.178
<i>Rhopalonema velatum</i> <sup>h</sup>	0.620	0.635	0.525	0.528	0.016	0.230
<i>Sminthea eurygaster</i> <sup>h</sup>	0.692	0.155	0.059	0.952	0.392	0.155
<i>Solmundella bitentaculata</i> <sup>h</sup>	0.285	0.627	0.237	<0.001***	0.451	0.120
<i>Eirene hexanemalis</i> <sup>m</sup>	0.014*	0.086	0.289	0.037*	0.355	0.740
<i>Abylopsis eschscholtzi</i> <sup>s</sup>	0.053	0.074	<0.001***	0.015*	0.566	0.114
<i>Abylopsis tetragona</i> <sup>s</sup>	0.180	0.510	0.720	0.009**	0.430	0.118
<i>Bassia bassensis</i> <sup>s</sup>	0.800	0.743	0.027*	0.568	0.090	0.186
<i>Chelophyes appendiculata</i> <sup>s</sup>	0.010*	0.184	0.563	0.487	0.252	0.230
<i>Diphyes chamissonis</i> <sup>s</sup>	0.237	0.674	0.009**	0.044*	0.467	0.223
<i>Eudoxoides mitra</i> <sup>s</sup>	0.401	0.859	0.433	0.139	0.174	0.197
<i>Eudoxoides spiralis</i> <sup>s</sup>	0.002**	0.027*	0.256	0.296	0.262	0.145
<i>Lensia meteor</i> <sup>s</sup>	0.270	0.962	0.747	0.256	0.299	0.087
<i>Lensia subtilis</i> <sup>s</sup>	0.094	0.193	0.160	0.004**	0.239	0.100
<i>Lensia subtiloides</i> <sup>s</sup>	0.274	0.072	0.339	0.004**	0.651	0.181
<i>Sulculeolaria chuni</i> <sup>s</sup>	0.006*	0.235	0.180	0.189	0.369	0.164

\*\*\*P < 0.001; \*\*P < 0.01; \*P < 0.05. h, holoplanktonic hydromedusae; m, meroplanktonic hydromedusae; s, siphonophore.





are holoplanktonic and are widely found in the neritic and the oceanic regions (Pavez et al., 2010). Thus, the species number of holoplanktonic hydromedusae and siphonophore may not be affected by the wind-driven jet in the present study.

Generally, the medusae abundance was influenced by environmental factors, such as temperature, salinity, oxygen concentration, and food sources (Pagès et al., 1996; Pavez et al., 2010; Haberlin et al., 2019). Temperature is identified as one of the most important factors in the distribution of medusae (Buecher and Gibbons, 2000; Pavez et al., 2010). For example, Pagès and Gili (1991) have suggested that in the Benguela upwelling ecosystem, dense aggregations of medusae were collected in the warm waters of the vicinity of the front zone. Conversely, the GAM analyses indicated that in contrast to diet, the temperature was not significantly correlated with the distribution of medusae (Table 3 and Figure 6). The nutrient-rich coastal water was carried into the WJR, causing higher phytoplankton density in the WJR than that in adjacent waters (Liu et al., 2012; Lu et al., 2018; Chen et al., 2021) and supporting high zooplankton biomass (Thibault et al., 1994). As a carnivorous predator with a broad zooplanktivorous diet (Pavez et al., 2010; Haberlin et al., 2019), the abundance of medusae increases due to the elevated chlorophyll concentration and zooplankton biomass in the WJR (Coyle and Cooney, 1993). Therefore, in this study, the increase of Chl *a* and diet in the WJR resulted in high medusae abundance.

Additionally, the study of Haberlin et al. (2019) has found that like the zooplankton biomass, the abundance of cnidarians was higher in the Celtic Sea Front than that in the adjacent regions, and this finding is similar to the results of the present study. However, the biomasses of cnidarians in the Southern Ocean in the Antarctic Polar Frontal Zone and the vicinity region were not significantly different (Pagès et al., 1996). The possible reason is that as the nutrients were high in the Southern Ocean, the coastal waters do not greatly promote the increase of chlorophyll concentration and the food biomass, thereby causing a similar abundance of medusae between the front zone and adjacent regions. Compared with the Southern Ocean, the diet and the medusae abundance in the WJR have strongly responded to increasing Chl *a* concentration due to the oligotrophic condition in the SCS in this study.

The abundances of holoplanktonic hydromedusae and siphonophore in the WJR were higher than those in the NWJR (Supplementary Table 1 and Figure 7). The larvae of holoplanktonic hydromedusae (Narcomedusae and Trachymedusae) species develop directly into medusae adults with no polyp stage. The coastal water with high Chl *a* concentration improved the diet in the WJR, thereby providing rich food sources for these species and causing high abundance (Supplementary Table 1). For example, the abundance of *A. hemistoma* (Trachymedusae) and *S. bitentaculata* (Narcomedusae) were significantly influenced by diet in

accordance with the GAM analyses (Table 3), and these abundances increased with increasing diet. A previous study showed that the abundances of *A. hemistoma* and *L. tetraphylla* were significantly improved by the upwelling, including high Chl *a* concentration and food organisms in the Benguela ecosystem (Pagès and Gili, 1991). As for the meroplanktonic hydromedusae, the total abundance showed no significant difference between the WJR and the NWJR (Table 1). Thus, the increase in diet did not increase the meroplanktonic medusae abundance in WJR because the meroplanktonic medusae cannot reproduce in oceanic regions. In terms of the siphonophore, these abundances in the WJR and the NWJR have no significant difference, but the abundance was high in the WJR due to the influence of the coastal waters (Table 2 and Figure 5).

In terms of the vertical distribution, medusae at three transects were substantially affected by the thermocline (Figure 5). They were mainly distributed above the thermocline, and showed no remarkable diel vertical migration both in the WJR and NWJR. The vertical distribution of medusae influenced by the thermocline is a universal phenomenon and well recorded in different marine ecosystems (Pagès and Gili, 1991; Lučić et al., 2009; Júnior et al., 2015). Additionally, the medusae abundance in the WJR and the NWJR have significant differences above the thermocline, whereas their abundance below the thermocline was similar, indicating that the coastal water with low-salinity and nutrient-rich mainly affected the abundance of medusae above the thermocline in WJR.

## CONCLUSION

The medusae community in the WJR was significantly influenced by the wind-driven jet (Figure 7). The species number of meroplanktonic hydromedusae in the WJR was higher than that in the NWJR due to the coastal species transported by the southwest wind jet and the anticyclonic eddy. Nutrient-rich coastal water improved the Chl *a* concentration in the WJR, supporting a high diet, and resulting in an increased abundance of holoplanktonic hydromedusae and siphonophore. Additionally, in the WJR, only the abundance of medusae above the thermocline was affected by the coastal water, while medusae below the thermocline between the WJR and the NWJR showed no significant difference. GAM analyses showed that the diet was the most important factor affecting the distribution of holoplanktonic hydromedusae and siphonophore,

## REFERENCES

- Aristegui, J., Barton, E. D., Álvarez-Salgado, X. A., Santos, A. M. P., Figueiras, F. G., Kifani, S., et al. (2009). Sub-regional ecosystem variability in the Canary current upwelling. *Prog. Oceanogr.* 83, 33–48. doi: 10.1016/j.pocean.2009.07.031
- Brock, M. A., and Strehler, B. L. (1963). Studies on the comparative physiology of aging. IV. Age and mortality of some marine Cnidaria in the laboratory. *J. Gerontol.* 18, 23–28. doi: 10.1093/geronj/18.1.23
- Brodeur, R. D., Suchman, C. L., Reese, D. C., Miller, T. W., and Daly, E. A. (2008). Spatial overlap and trophic interactions between pelagic fish and large jellyfish in the northern California current. *Mar. Biol.* 154, 649–659. doi: 10.1007/s00227-008-0958-3

whereas meroplanktonic hydromedusae were influenced by the combination of temperature, salinity, and diet.

## DATA AVAILABILITY STATEMENT

The original contributions presented in the study are included in the article/Supplementary Material, further inquiries can be directed to the corresponding author.

## AUTHOR CONTRIBUTIONS

RG measured biomass and wrote the original draft. HC helped with data analysis and interpretation, and fundamental help in developing the manuscript. HC and LL classified medusae organisms. GL supervised the project related to this study and fundamental help in data analysis and interpretation. LW measured nutrient concentration. XL measured chlorophyll-concentration. BH, YZ, and XL helped to revise the work. All authors contributed to the article and approved the submitted version.

## FUNDING

This work was supported by the National Key Research and Development Program of China (No. 2016YFA0601202) and National Natural Science Foundation of China (No. 42076146).

## ACKNOWLEDGMENTS

We are grateful to the crew members of “Dong Fang Hong 2” for their assistance and Yousong Huang, Jing Fang, and Xiaoyan Yi for their help in collecting samples. We are also grateful to the two reviewers for the highly constructive comments that improved the manuscript.

## SUPPLEMENTARY MATERIAL

The Supplementary Material for this article can be found online at: <https://www.frontiersin.org/articles/10.3389/fmars.2021.760371/full#supplementary-material>

- Buecher, E., and Gibbons, M. J. (2000). Interannual variation in the composition of the assemblages of medusae and ctenophores in St Helena Bay, Southern Benguela Ecosystem. *Sci. Mar.* 64, 123–134. doi: 10.3989/scimar.2000.64s1123
- Campbell, J. W. (1995). The lognormal distribution as a model for bio-optical variability in the sea. *J. Geophys. Res. Oceans* 100, 13237–13254. doi: 10.1029/95JC00458
- Chen, C. S., Lai, Z. G., Beardsley, R. C., Xu, Q. H., Lin, H. C., and Viet, N. T. (2012). Current separation and upwelling over the southeast shelf of Vietnam in the South China Sea. *J. Geophys. Res. Oceans* 117:C03033. doi: 10.1029/2011JC007150
- Chen, G. X., Xiu, P., and Chai, F. (2014). Physical and biological controls on the summer chlorophyll bloom to the east of Vietnam. *J. Oceanogr.* 70, 323–328. doi: 10.1007/s10872-014-0232-x

- Chen, Y., Shi, H. Y., and Zhao, H. (2021). Summer phytoplankton blooms induced by upwelling in the Western South China Sea. *Front. Mar. Sci.* 8:740130. doi: 10.3389/fmars.2021.740130
- Clarke, K. R. (1993). Non-parametric multivariate analyses of changes in community structure. *Aust. J. Ecol.* 18, 117–143. doi: 10.1111/j.1442-9993.1993.tb00438.x
- Coyle, K. O., and Cooney, R. T. (1993). Water column sound-scattering and hydrography around the Pribilof Islands, Bering Sea. *Cont. Shelf Res.* 13, 803–827. doi: 10.1016/0278-4343(93)90028-V
- Da, N. D., Herrmann, M., Morrow, R., Nino, F., Huan, N. M., and Trinh, N. Q. (2019). Contributions of wind, ocean intrinsic variability, and ENSO to the inter annual variability of the South Vietnam upwelling: a modeling study. *J. Geophys. Res. Oceans* 124, 6545–6574. doi: 10.1029/2018JC014647
- Duran-Campos, E., Salas-de-Leon, D., Monreal-Gomez, M., Ideco-Ramirez, J., and Coria-Monter, E. (2015). Differential zooplankton aggregation due to relative vorticity in a semi-enclosed bay. *Estuar. Coast. Shelf Sci.* 164, 10–18.
- Fang, W. D., Guo, Z. X., and Huang, Y. T. (1997). The observational study of the ocean circulation in the southern South China Sea. *Chin. Sci. Bull.* 42, 2264–2271. (in Chinese),
- Field, J. G., Clark, K. R., and Warwick, R. M. (1982). A practical strategy for analysing multispecies distribution patterns. *Mar. Ecol. Prog. Ser.* 8, 37–52.
- George, J. A., Lonsdale, D. J., Merlo, L. R., and Gobler, C. J. (2015). The interactive roles of temperature, nutrients, and zooplankton grazing in controlling the winter-spring phytoplankton bloom in a temperate, coastal ecosystem, Long Island Sound. *Limnol. Oceanogr.* 60, 110–126. doi: 10.1002/lno.10020
- Graham, W. M., Pagès, F., and Hamner, W. M. (2001). A physical context for gelatinous zooplankton aggregations: a review. *Hydrobiologia* 451, 199–212. doi: 10.1023/A:1011876004427
- Grasshoff, K., Ehrardt, M., and Kremling, K. (1983). *Methods of Seawater Analysis*, 2nd Edn. Weinheim: Verlag Chemie.
- Haberlin, D., Raine, R., McAllen, R., and Doyle, T. K. (2019). Distinct gelatinous zooplankton communities across a dynamic shelf sea. *Limnol. Oceanogr.* 64, 1802–1818. doi: 10.1002/lno.11152
- Huang, X. L., Jing, Z. Y., Zheng, R. X., and Cao, H. J. (2020). Dynamical analysis of submesoscale fronts associated with wind-forced offshore jet in the western South China Sea. *Acta Oceanol. Sin.* 39, 1–12. doi: 10.1007/s13131-020-1671-4
- Júnior, M. N., Brandini, F. P., and Codina, J. C. U. (2015). Diel vertical dynamics of gelatinous zooplankton (Cnidaria, Ctenophora and Thaliacea) in a subtropical stratified ecosystem (South Brazilian Bight). *PLoS One* 10:e144161. doi: 10.1371/journal.pone.0144161
- Ke, Z. X., Tan, Y. H., Huang, L. M., Zhang, J. L., and Lian, S. M. (2012). Relationship between phytoplankton composition and environmental factors in the surface waters of southern South China Sea in early summer of 2009. *Acta Oceanol. Sin.* 31, 109–119. doi: 10.1007/s13131-012-0211-2
- Kideys, A., and Romanova, Z. (2001). Distribution of gelatinous macrozooplankton in the southern Black Sea during 1996–1999. *Mar. Biol.* 139, 535–547. doi: 10.1007/s002270100602
- Kitajima, S., Iguchi, N., Honda, N., Watanabe, T., and Katoh, O. (2015). Distribution of *Nemopilema nomurai* in the southwestern Sea of Japan related to meandering of the Tsushima warm current. *J. Oceanogr.* 71, 287–296. doi: 10.1007/s10872-015-0288-2
- Kuo, N. J., Zheng, Q., and Ho, C. R. (2000). Satellite observation of upwelling along the western coast of the South China Sea. *Remote Sens. Environ.* 74, 463–470. doi: 10.1016/S0034-4257(00)00138-3
- Li, J., Wang, G., and Zhai, X. (2017). Observed cold filaments associated with mesoscale eddies in the South China Sea. *J. Geophys. Res. Oceans* 122, 762–770. doi: 10.1002/2016JC012353
- Li, Y. L., Han, W. Q., Wilkin, J. L., Zhang, W. F., Arango, H., Zavala-Garay, J., et al. (2014). Interannual variability of the surface summertime eastward jet in the South China Sea. *J. Geophys. Res. Oceans* 119, 7205–7228. doi: 10.1002/2014JC010206
- Liu, H. J., Zhu, M. L., Guo, S. J., Zhao, X. H., and Sun, X. X. (2020). Effects of an anticyclonic eddy on the distribution and community structure of zooplankton in the South China Sea northern slope. *J. Mar. Syst.* 205:103311. doi: 10.1016/j.jmarsys.2020.103311
- Liu, X., Wang, J., Cheng, X. H., and Du, Y. (2012). Abnormal upwelling and chlorophyll-a concentration off South Vietnam in summer 2007. *J. Geophys. Res. Oceans* 117:C07021. doi: 10.1029/2012JC008052
- Lu, W. F., Oey, L. Y., Liao, E. H., Zhuang, W., Yan, X. H., and Jiang, Y. W. (2018). Physical modulation to the biological productivity in the summer Vietnam upwelling system. *Ocean Sci.* 14, 1303–1320. doi: 10.5194/os-14-1303-2018
- Lučić, D., Benović, A., Morović, M., Batišić, M., and Onofri, I. (2009). Diel vertical migration of medusae in the open Southern Adriatic Sea over a short time period (July 2003). *Mar. Ecol. Prog. Ser.* 30, 16–32. doi: 10.1111/j.1439-0485.2008.00264.x
- Luo, J. Y., Grassian, B., Tang, D., Irisson, J. O., Greer, A. T., Guigand, C. M., et al. (2014). Environmental drivers of the fine-scale distribution of a gelatinous zooplankton community across a mesoscale front. *Mar. Ecol. Prog. Ser.* 510, 129–149. doi: 10.3354/meps10908
- Lynam, C. P., Hay, S. J., and Brierley, A. S. (2005). Jellyfish abundance and climatic variation: contrasting responses in oceanographically distinct regions of the North Sea, and possible implications for fisheries. *J. Mar. Biol. Assoc. U. K.* 85, 435–450. doi: 10.1017/S0025315405011380
- Metzger, E. J. (2003). Upper ocean sensitivity to wind forcing in the South China Sea. *J. Oceanogr.* 59, 783–798. doi: 10.1023/B:JOCE.0000009570.41358.c5
- Miglietta, M. P., Rossi, M., and Collin, R. (2008). Hydromedusa blooms and upwelling events in the Bay of Panama, Tropical East Pacific. *J. Plankton Res.* 30, 783–793. doi: 10.1093/plankt/fbn038
- Mills, C. E. (1993). Natural mortality in NE Pacific coastal hydromedusae: grazing predation, wound healing and senescence. *Bull. Mar. Sci.* 53, 194–203. doi: 10.1029/93JC01662
- Ngo, M. H., and Hsin, Y. C. (2021). Impacts of wind and current on the interannual variation of the summertime upwelling off southern Vietnam in the South China Sea. *J. Geophys. Res. Oceans* 126:e2020JC016892. doi: 10.1029/2020JC016892
- Ning, X., Chai, F., Xue, H., Cai, Y., Liu, C., and Shi, J. (2004). Physical-biological oceanographic coupling influencing phytoplankton and primary production in the South China Sea. *J. Geophys. Res. Oceans* 109:C10005. doi: 10.1029/2005JC002968
- Pagès, F., and Gili, J. M. (1991). Effects of large-scale advective processes on gelatinous zooplankton populations in the northern Benguela ecosystem. *Mar. Ecol. Prog. Ser.* 75, 202–215. doi: 10.3354/meps075205
- Pagès, F., and Gili, J. M. (1992). Influence of Agulhas waters on the population structure of planktonic cnidarians in the southern Benguela region. *Sci. Mar.* 56, 109–123. doi: 10.1186/1710-1492-6-S3-P33
- Pagès, F., White, M. G., and Rodhouse, P. G. (1996). Abundance of gelatinous carnivores in the nekton community of the Antarctic Polar Frontal Zone in summer 1994. *Mar. Ecol. Prog. Ser.* 141, 139–147. doi: 10.3354/meps141139
- Pavez, M. A., Landaeta, M. F., Castro, L. R., and Schneider, W. (2010). Distribution of carnivorous gelatinous zooplankton in the upwelling zone off central Chile (austral spring 2001). *J. Plankton Res.* 32, 1051–1065. doi: 10.1093/plankt/fbq029
- Pedersen, O. P., Tande, K. S., Li, C. L., and Zhou, M. (2010). Restructuring of a zooplankton community by perturbation from a wind-forced coastal jet. *Oceanologia* 52, 473–497. doi: 10.5697/oc.52-3.473
- Purcell, J. E., and Arai, M. N. (2001). Interactions of pelagic cnidarians and ctenophores with fish: a review. *Hydrobiologia* 451, 27–44. doi: 10.1023/A:1011883905394
- Purcell, J. E., and Sturdevant, M. V. (2001). Prey selection and dietary overlap among zooplanktivorous jellyfish and juvenile fishes in Prince William Sound, Alaska. *Mar. Ecol. Prog. Ser.* 210, 67–83. doi: 10.3354/meps210067
- Purcell, J. E., Uye, S. I., and Lo, W. T. (2007). Anthropogenic causes of jellyfish blooms and their direct consequences for humans: a review. *Mar. Ecol. Prog. Ser.* 350, 153–174. doi: 10.3354/meps07093
- Rodriguez, C. S., Marques, A. C., Mianzan, H. W., Tronolone, V. B., Migotto, A. E., and Genzano, G. N. (2017). Environment and life cycles influence distribution patterns of hydromedusae in austral South America. *Mar. Biol. Res.* 13, 1–12. doi: 10.1080/17451000.2017.1280170
- Rosen-Runge, E. C. (1970). Life cycle of the hydromedusae *Phialidium gregarium* (A. Agassiz, 1862) in the laboratory. *Biol. Bull.* 139, 203–211. doi: 10.2307/1540137
- Sevadjian, J. C., Mcmanus, M. A., Ryan, J., Greer, A. T., Cowen, R. K., and Woodson, C. B. (2014). Across-shore variability in plankton layering and abundance associated with physical forcing in Monterey Bay, California. *Cont. Shelf Res.* 72, 138–151. doi: 10.1016/j.csr.2013.09.018

- Sun, Y., and Lan, J. (2021). Summertime eastward jet and its relationship with western boundary current in the South China Sea on the interannual scale. *Clim. Dyn.* 56, 935–947. doi: 10.1007/s00382-020-05511-z
- Thibault, D., Gaudy, R., and Lefevre, J. (1994). Zooplankton biomass, feeding and metabolism in a geostrophic frontal area (Almeria-Oran Front, western Mediterranean)-Significance to pelagic food webs. *J. Mar. Syst.* 5, 297–311. doi: 10.1016/0924-7963(94)90052-3
- Voynova, Y. G., Oliver, M. J., and Sharp, J. H. (2013). Wind to zooplankton: ecosystem-wide influence of seasonal wind-driven upwelling in and around the Delaware Bay. *J. Geophys. Res. Oceans* 118, 6437–6450. doi: 10.1002/2013JC008793
- Wang, J., and Tang, D. L. (2014). Phytoplankton patchiness during spring intermonsoon in western coast of South China Sea. *Deep Sea Res. Part II* 101, 120–128. doi: 10.1016/j.dsr2.2013.09.020
- Wang, Y., Yu, Y., Zhang, Y., Zhang, H. R., and Chai, F. (2020). Distribution and variability of sea surface temperature fronts in the South China Sea. *Estuar. Coast. Shelf Sci.* 240:106793. doi: 10.1016/j.ecss.2020.10.6793
- Wilkin, R. T., McNeil, M. S., Adair, C. J., and Wilson, J. T. (2001). Field measurement of dissolved oxygen: a comparison of methods. *Ground Water Monit. Remediat.* 21, 124–132. doi: 10.1111/j.1745-6592.2001.tb00648.x
- Wood, S. N. (2006). *Generalized Additive Models: An introduction with R*. London: Chapman & Hall.
- Woodson, C. B., and Litvin, S. Y. (2015). Ocean fronts drive marine fishery production and biogeochemical cycling. *Proc. Natl. Acad. Sci. U.S.A.* 112, 1710–1715. doi: 10.1073/pnas.1417143112
- Xie, S. P., Chang, C. H., Xie, Q., and Wang, D. X. (2007). Intraseasonal variability in the summer South China Sea: wind jet, cold filament, and recirculations. *J. Geophys. Res. Oceans* 112:C10008. doi: 10.1029/2007JC004238
- Xie, S. P., Xie, Q., Wang, D. X., and Liu, W. T. (2003). Summer upwelling in the South China Sea and its role in regional climate variations. *J. Geophys. Res. Oceans* 108:3261. doi: 10.1029/2003JC001867
- Zhao, H., Zhao, J., Sun, X., Chen, F., and Han, G. (2018). A strong summer phytoplankton bloom southeast of Vietnam in 2007, a transitional year from El Nino to La Nina. *PLoS One* 13:e189926. doi: 10.1371/journal.pone.0189926

**Conflict of Interest:** The authors declare that the research was conducted in the absence of any commercial or financial relationships that could be construed as a potential conflict of interest.

**Publisher's Note:** All claims expressed in this article are solely those of the authors and do not necessarily represent those of their affiliated organizations, or those of the publisher, the editors and the reviewers. Any product that may be evaluated in this article, or claim that may be made by its manufacturer, is not guaranteed or endorsed by the publisher.

Copyright © 2021 Ge, Chen, Li, Liu, Huang, Wang, Zhuang and Liu. This is an open-access article distributed under the terms of the Creative Commons Attribution License (CC BY). The use, distribution or reproduction in other forums is permitted, provided the original author(s) and the copyright owner(s) are credited and that the original publication in this journal is cited, in accordance with accepted academic practice. No use, distribution or reproduction is permitted which does not comply with these terms.